

# AnoVL: Adapting Vision-Language Models for Unified Zero-shot Anomaly Localization

Hanqiu Deng, Zhaoxiang Zhang, Jinan Bao, Xingyu Li

University of Alberta

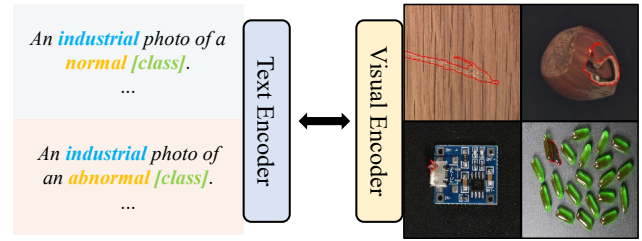
## Abstract

Contrastive Language-Image Pre-training (CLIP) models have shown promising performance on zero-shot visual recognition tasks by learning visual representations under natural language supervision. Recent studies attempt the use of CLIP to tackle zero-shot anomaly detection by matching images with normal and abnormal state prompts. However, since CLIP focuses on building correspondence between paired text prompts and global image-level representations, the lack of patch-level vision to text alignment limits its capability on precise visual anomaly localization. In this work, we introduce a training-free adaptation (TFA) framework of CLIP for zero-shot anomaly localization. In the visual encoder, we innovate a training-free value-wise attention mechanism to extract intrinsic local tokens of CLIP for patch-level local description. From the perspective of text supervision, we particularly design a unified domain-aware contrastive state prompting template. On top of the proposed TFA, we further introduce a test-time adaptation (TTA) mechanism to refine anomaly localization results, where a layer of trainable parameters in the adapter is optimized using TFA’s pseudo-labels and synthetic noise-corrupted tokens. With both TFA and TTA adaptation, we significantly exploit the potential of CLIP for zero-shot anomaly localization and demonstrate the effectiveness of our proposed methods on various datasets.

## Introduction

Visual anomaly detection and localization is a pivotal topic of computer vision, evident in its diverse applications across industrial visual inspection (Bergmann et al. 2019; Zou et al. 2022), video surveillance (Liu et al. 2018), and medical diagnosis (Schlegl et al. 2019). This intricate and fine-grained task involves the detection and localization of atypical patterns, anomalies, or deviations within visual data. Its complexity nature mainly stems from the inherent diversity of anomalies. For instance, many anomalies manifest as subtle deviations in texture, color, shape, or motion, blending seamlessly into the surrounding normal samples (Bergmann et al. 2019; Zou et al. 2022).

Prior arts in anomaly detection and localization focus on training a dedicated model for each category of normal images (Liu et al. 2023; Roth et al. 2022; Deng and Li 2022; Bergmann et al. 2020; Zavrtnik, Kristan, and



Unified Zero-shot Anomaly Localization

Figure 1: The paradigm of zero-shot anomaly localization. Our adapted vision-language models can detect anomalies from any object. The anomaly score is derived from the distance between textural and visual tokens.

Skočaj 2021). However, training category-specific models is undoubtedly costly in real-world scenarios. Recently, impressive progress has been made towards unified models for multi-class anomaly detection, aiming to establish a single model capable of identifying multi-class anomalies uniaid,regad. Nonetheless, these advancements are still limited to modeling normal distributions on known categories and fail in detecting anomalies in unknown or open-set scenarios. In this study, we tackle an open-world anomaly detection problem, which is to identify and locate anomalies on unknown classes of samples in a zero-shot manner.

Recent CLIP models have shown promising properties for detecting unknown objects (Gu et al. 2021; Kuo et al. 2022) as well as out-of-distribution data (Ming et al. 2022; Cohen, Abutbul, and Hoshen 2022). By learning on millions of image-text pairs, CLIP has excellent zero-shot transfer capability for downstream tasks. In this study, we aim to achieve precise zero-shot anomaly localization with CLIP. To this end, two challenges in CLIP have to be well addressed. First, anomaly detection is a fine-grained task where the discriminative details are too subtle to be well represented by CLIP. Second, CLIP presents limited local descriptors due to its training on paring image-wise global features and text embedding. This becomes an obstacle to precisely locating anomalous regions.

To tackle such issues, we propose a novel framework in Fig. 1 for adapting CLIP to zero-shot anomaly localization.

Briefly, our framework consists of a pretrained CLIP model, a training-free adaptation module, and a test-time adaptation mechanism. Two innovations contribute to our **training-free adaptation (TFA)**. On one hand, we are concerned with constructing local representations from the pretrained visual model of CLIP. Prior studies show that image-level representations usually originate from the global average pooling operation and CLIP shows proper dense prediction via eliminating attention pooling (Zhou et al. 2016; Zhou, Loy, and Dai 2022; Li et al. 2023). Inspired by this insight, we extract values from the visual encoder and propose to utilize a novel training-free value-to-value (V-V) attention to compute the local-aware patch tokens. On the other hand, as the zero-shot recognition capability of CLIP depends on the quality of textual prompts (Radford et al. 2021; Jeong et al. 2023), we hypothesize that fine-grained detection can benefit from a more precise prompt design and propose a unified domain-aware contrastive state prompt template,

A [domain] photo of a [state] [class],

for generating exhaustive prompts. The contrastive state words enable the model to robustly distinguish between normal and abnormal features, and domain-aware prompts encourage textual tokens to adapt to the visual feature space. To further improve the zero-shot generalization ability of CLIP, we propose a novel fast **test-time adaptation (TTA)** mechanism for anomaly localization. Our TTA incorporates a learn-able residual-like adapter to tailor patch tokens obtained from TFA for specific queries. By jointly optimized with two discriminative tasks on TFA’s pseudo-labels and synthetic noise-corrupted tokens, the proposed adapter greatly improves the performance of zero-shot anomaly localization and leverages a proper trade-off between performance and cost. Extensive experiments on MVTecAD (Bergmann et al. 2019) and VisA (Zou et al. 2022) demonstrate the remarkable superiority of our method under the uniform zero-shot anomaly detection and localization setting. We also conduct comprehensive ablation studies to demonstrate the effectiveness of our framework.

## Related Work

**Vision-Language Models.** As data scale increases, pretrained visual language models present significant achievements in downstream tasks (Chen et al. 2020; Desai and Johnson 2021; Joulin et al. 2016; Radford et al. 2021). The CLIP models (Radford et al. 2021), derived from contrastive vision language pre-training on millions of image-text pairs gathered from the internet, showcases a profound generality, whereby its prompt-driven zero-shot inference exhibits superior ability for identifying unseen images (Zhou et al. 2022a). Recent studies expand the zero-shot transfer-ability of CLIP models to open-vocabulary semantic segmentation by extracting the intrinsic dense features (Zhou, Loy, and Dai 2022; Shin, Xie, and Albanie 2022; Li et al. 2023). Some efforts have made considerable progress in improving the recognition performance of CLIP, such as the prompt engineering (Zhou et al. 2022b,a; Shu et al. 2022), the adapter module (Gao et al. 2021; Zhang et al. 2021), etc. Notably, CLIP can naturally detect out-of-distribution data without

any further training, which inspired us to use CLIP for zero-shot anomaly detection and localization.

**Anomaly Detection & Localization** Most existing anomaly detection methods rely on modeling the distribution of normal samples to identify anomalies (Defard et al. 2021; Roth et al. 2022; Deng and Li 2022; You et al. 2022), whereby prevalent anomaly detection benchmarks typically provide normal-only datasets for training (Bergmann et al. 2019; Zou et al. 2022). In particular, robust anomaly detection models often tend to rely on visual models (He et al. 2016; Zagoruyko and Komodakis 2016; Dosovitskiy et al. 2020) pre-trained on large-scale image datasets (Deng et al. 2009). These methods locate anomalies by comparing samples with normal features obtained by reconstruction (Salehi et al. 2021a; Deng and Li 2022; You et al. 2022), caching (Roth et al. 2022; Defard et al. 2021), etc. A further challenge is the unified anomaly detection model, which concerns using one model to detect anomalies in multi-class images (Huang et al. 2022; You et al. 2022). For the zero-shot setting, some methods attempt to detect internal anomalies using the natural structure of the image (Aota, Tong, and Okatani 2023; Schwartz et al. 2022). Recently, WinCLIP (Jeong et al. 2023) is proposed to process images by multi-scale window moving and classify each window with CLIP. However, WinCLIP is time-consuming because the visual coder performs extra processing of multi-scale windowed image patches. In contrast to WinCLIP, our framework extracts the intrinsic dense features directly from CLIP to locate anomalies is absolutely efficient.

## Methodology

In this section, we first introduce the CLIP-based baseline model for zero-shot anomaly detection and localization. Then, we elaborate the proposed training-free adaptation, which includes the V-V attention for local-aware token calculation and a domain-aware state prompt template for better vision-language alignment. Lastly, we specify our test-time adaptation mechanism to enhance anomaly localization. Fig. 2 depicts the overview of our framework for zero-shot anomaly localization.

### CLIP for Zero-shot Anomaly Recognition

Let’s first briefly review the zero-shot visual recognition ability of CLIP. CLIP includes a visual coder and a text encoder to extract visual features and text features respectively. Given a comprehensive multi-million dataset of image-text pairs, CLIP trains both encoders by maximizing the feature cosine similarity between images and their corresponding text, which empowers CLIP to align an image with any text in the open vocabulary. For any class in testing, we define a text that includes the concept of this target, e.g. ”a photo of a [CLASS]”. Specifically, given an unknown image and a pre-defined text, the visual encoder and the text encoder output the visual class token  $v \in R^C$  and the text token  $t \in R^C$ , respectively. Here,  $C$  represents the feature dimension. The cosine distance between  $v$  and  $t$ , denoted by  $\langle v, t \rangle$ , quantifies the similarity between the image and the class concept.

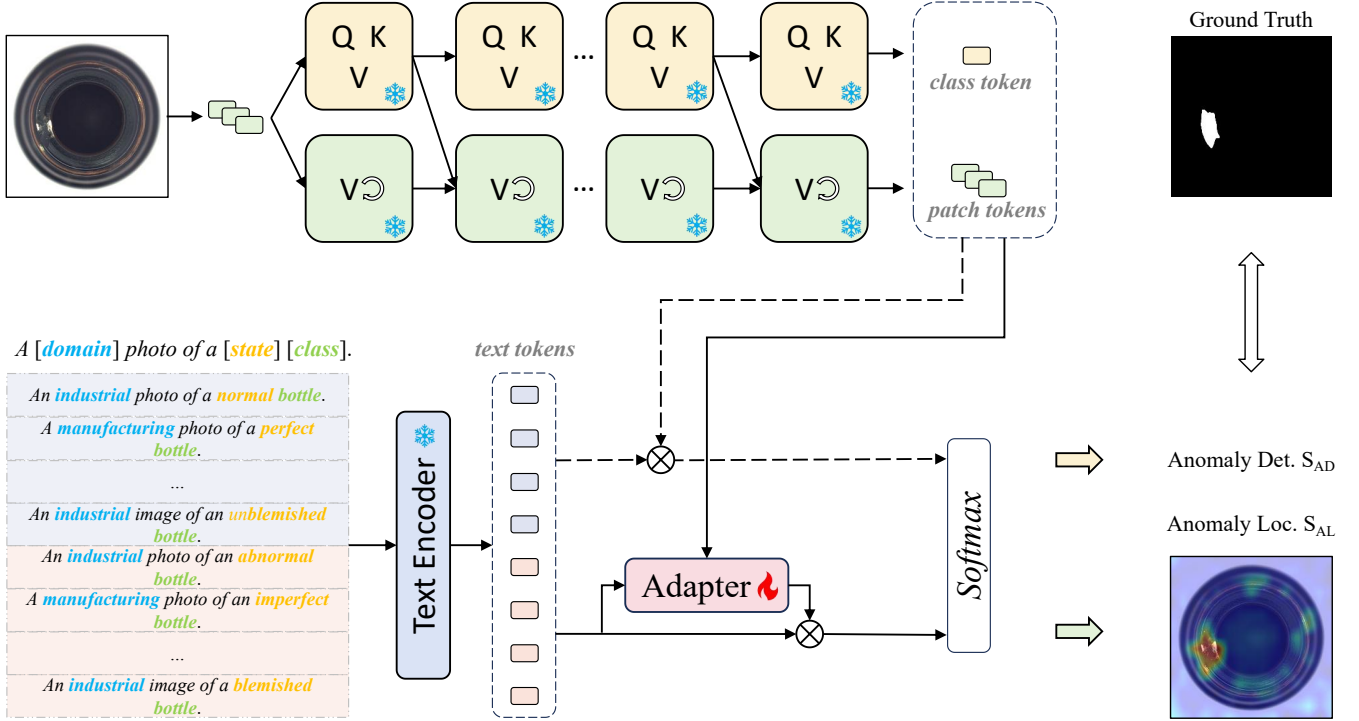


Figure 2: Overview of our framework for zero-shot anomaly localization. The dash line indicates our TFA prediction and the solid line indicates the our TTA prediction. The snow denotes the frozen module and the flame denotes the optimized module.

Anomaly detection involves the semantic concepts of "normal" and "anomaly", so for a test class we can simply define two textual prompts i.e. "a photo of a normal [CLASS]" and "a photo of an abnormal [CLASS]", and extract the corresponding text tokens  $[t^+, t^-]$ . Given a test image and the corresponding visual token, the probability for anomaly detection is computed as

$$S_{AD}(v) = \frac{\exp(\langle v, t^- \rangle)}{\exp(\langle v, t^+ \rangle) + \exp(\langle v, t^- \rangle)}. \quad (1)$$

Note that no knowledge of visual anomaly is injected into the model, but rather unknown anomalies are detected through the powerful open-world generalization of CLIP.

Although CLIP is only trained to match the global content of an image with text, the final layer of the visual encoder has a set of patch tokens  $P = \{p_1, \dots, p_M | p_i \in R^C\}$  that potentially contain image local information in the patch level. For a patch token  $p_i$ , the local anomaly score is computed as:

$$S_{AL}(p_i) = \frac{\exp(\langle p_i, t^- \rangle)}{\exp(\langle p_i, t^+ \rangle) + \exp(\langle p_i, t^- \rangle)}. \quad (2)$$

For an image with  $M$  patches split by the visual encoder, the  $M$  local anomaly scores are reorganized and up-sampled to align with the original size of the image for a final abnormality map. Note, in such a trivial anomaly localization strategy as a baseline, a lack of alignment between local patch tokens and text embedding leads to limited performance on locating anomalous regions.

## Training-free Adaptation (TFA)

**Local-aware token computation via value-to-value attention.** The Q-K-V attention mechanism of the visual transformer evenly predisposes patch tokens to characterize global features, since CLIP learns from image-text comparisons at the global level. To extract informative local features from the visual transformer, we carefully modify the attention so as to obtain local patch tokens without any further training. The original Q-K-V attention recipe consists of a layer norm (LN), a Q-K-V projection layer (QKVProj.), an attention mechanism with a projection layer (Proj.), and a multi-layer perceptron (MLP). It can be formulated as:

$$Z^{l-1} = [v; p_1; \dots; p_M], \quad (3)$$

$$[Q^l, K^l, V^l] = QKVProj.(LN(Z^{l-1})), \quad (4)$$

$$Z^l = Proj.(Attention(Q^l, K^l, V^l)) + Z^{l-1}, \quad (5)$$

$$Z^l = MLP(Z^l) + Z^l. \quad (6)$$

Queries and keys in the attention mechanism play the role of associating contextual relations. Prior studies show that the Q-K retrieval mode in the last layer somehow acts as a global average pooling for visual global description (Zhou, Loy, and Dai 2022; Li et al. 2023). Through bypassing Q-K attention, the values of the last layer lead to local tokens strongly associated with the given text (which has been confirmed by our ablation in Table 3). To further improve specific locality in patch tokens, we propose an novel Value-to-Value self-attention followed by residual linking per layer to

enhance local tokens. Our V-V attention in the adapted  $l$ th layer of a visual transformer can be formulated as:

$$V^l = Proj.(Attention(V^{l-1}, V^{l-1}, V^{l-1})) + V^{l-1}. \quad (7)$$

Compared to the original Q-K-V attention in Eq. (3)-(6), V-V attention replaces queries and keys by values and removes the top MLP layer. The patch tokens taken from the last layer of the visual transformer are fed into Eq. (2) for local anomaly scores. Notably, the V-V attention is training-free and runs efficiently for zero-shot anomaly localization.

**Domain-aware State Prompting.** In contrast to traditional visual models, the predictions of visual language models are critically dominated by the semantic texts. Proper semantic prompts enable CLIP to adapt to a specific task setting with no further training. Especially, anomaly detection, a fine-grained visual recognition task, could benefit from more precise specific prompts. Artificially designing a perfect task-specific prompt sentence is nearly impossible or requires extensive effort, yet a well-designed template can automatically generate enough prompts to comprehensively cover task-related concepts. To this end, we decompose the prompting engineering for a given **class** of zero-shot anomaly localization into three parts: **base** prompts, **contrastive-state** prompts, and **domain-aware** prompts.

**Base** prompts are universal templates generated from the default prompt "a photo of a [class]" by varying the context, e.g. "a cropped photo of a [class]" and "a bright photo of a [class]". Experiments on CLIP show that the ensemble of multiple base templates boosts the performance of zero-shot classifier. Such observation suggests that the prompt engineering has a significant impact on the zero-shot transfer of CLIP; Particularly, the ensemble of multiple prompts enhances the robustness of the text-guided classifier.

**Contrastive-state** (CS) prompts emphasize the antagonistic concepts of normal and abnormal states. According to  $S_{AD}$  and  $S_{AL}$ , we compute a normalized anomaly score with a pair of antagonistic state tokens. Thus, a series of opposing state words, such as "perfect" vs. "imperfect" and "with flaw" vs. "without flaw", allow visual tokens to be matched with their preferred states. Especially, anomalies are assumed to be unknown, so we tend to choose common state words including "broken", "imperfect", etc. For specific anomalies that are known, the state words include detailed descriptions. For example, the "wood" dataset in MVTEC (Bergmann et al. 2019) includes the defect type of "hole", so the corresponding contrastive-state prompt could be "with a hole" vs. "without a hole".

**Domain-aware** (DA) prompting is proposed for bridging the domain gap between the CLIP and the downstream task. Images for fine-grained vision tasks are typically a specific distribution, such as industrial images used for visual inspection. To align the distribution of text tokens with visual tokens, we propose domain-aware prompt engineering to adapt prompts to specific domains. For example, "industrial photo" for industry products, and "textual photo" for textured structures. As opposed to domain-agnostic prompts, domain-aware prompt engineering eliminates the distribution shift with a non-parametric manner.

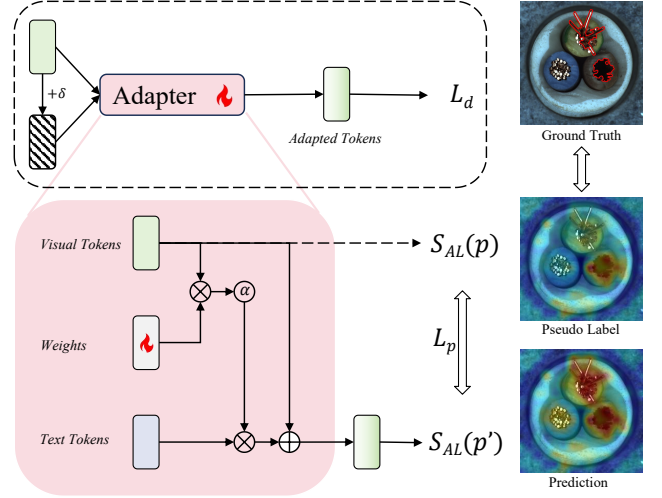


Figure 3: Detailed structure of our adapter. *Weights* denote the learnable parameters of the adapter. We use the noised patch tokens ( $+\sigma$ ) for discriminative loss  $L_d$  and the prediction  $S_{AL}(p)$  from TTA for pseudo-supervised loss.

Eventually, we summarize the elements that are beneficial to the prompting engineering into a unified template:

A [**domain**] photo of a [**state**] [**class**].

Based on this unified prompt template, we provide a few base prompt words and contrast state words and domain-aware words to generate massive prompters for zero-shot anomaly detection and localization. For normal text tokens  $[t_1^+, t_2^+, \dots, t_N^+]$  and abnormal text tokens  $[t_1^-, t_2^-, \dots, t_N^-]$  extracted from the prompts list, we compute the averaged tokens as the zero-shot anomaly detector in  $S_{AD}$  and  $S_{AL}$ :

$$t^+ = \frac{1}{N} \sum_i t_i^+, \quad t^- = \frac{1}{N} \sum_i t_i^-. \quad (8)$$

We show in experiments that such domain-aware state tokens  $[t_+, t_-]$  reliably improve the performance of zero-shot anomaly detection and localization.

### Test-time Adaptation (TTA)

Test-time adaptation is a technique adapting pre-trained models to downstream tasks in inference by optimizing few parameters (Shu et al. 2022). In this study, to further tailor the patch tokens for visual-language alignment in anomaly localization with respect to a specific query image, we design a non-linear residual-like adapter whose structure is shown in Fig. 3. Mathematically, we denote the set of text prompt tokens as  $T \in R^{2N \times C}$ , where  $t_i$  and  $t_{i+N}$  correspond to paired normal and abnormal tokens for  $0 < i \leq N$ . After obtaining the set of patch tokens  $P \in R^{M \times C}$  for a test image, the online-adapted patch token set can be written as:

$$P' = \alpha(P\omega^T)T + P, \quad (9)$$



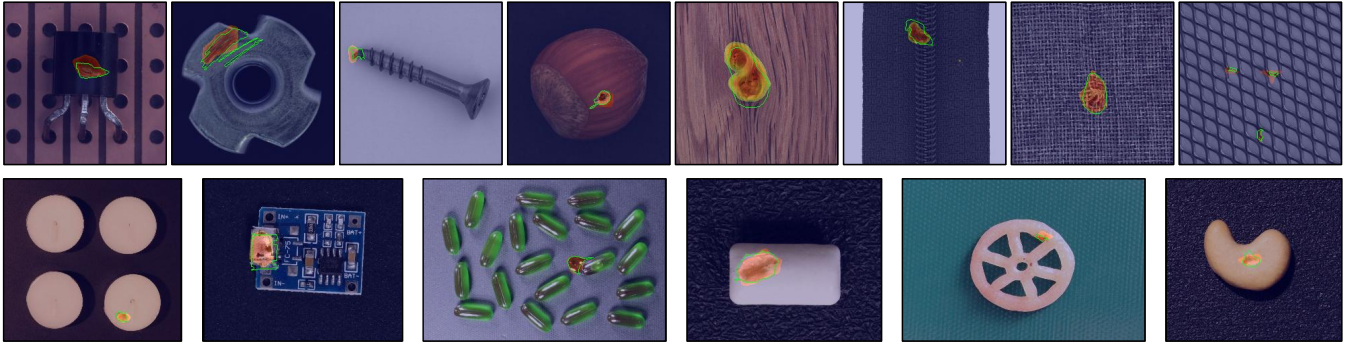


Figure 4: Visualization of zero-shot anomaly localization. The top row shows images from MVTEC and the bottom row shows images from VisA. The red mask refers to our prediction results while the green contour is the ground truth.

where  $\alpha$  is the softmax activation function and  $\omega \in R^{2N \times C}$  denotes the learn-able parameters initialized by the text tokens  $T$ . Notably, the proposed adaptor in Eq. (9) can be considered an attention operation taking  $P, \omega, T$  as Q, K and V, respectively. It enhances the alignment between text prompts and local patches by injecting state information in  $P'$ .

Optimizing the trainable parameter  $\omega$  in the adaptor involves in designing self-supervised tasks. Unlike traditional TTA relying on data-augmentation and multiple-pass of forward propagation (which is time-consuming for real-time anomaly localization), we propose to directly perturb visual tokens. Specifically, for adapted patch tokens  $P' = \{p'_1, \dots, p'_M\}$  from a query, we synthesize noise-corrupted tokens  $P'_{nc} = \{p'_1 + \delta_1, \dots, p'_M + \delta_M\}$ , where  $\delta_i \in R^C$  is Gaussian noise sampled from  $N(\mu, \sigma^2)$ . Based on  $P'$  and  $P'_{nc}$ , two self-supervised discriminative tasks are constructed to optimize  $\omega$ : **(1) To discriminate original and noise-corrupted tokens in  $P'$  and  $P'_{nc}$ .** A cross-entropy loss over the  $2M$  patch tokens,

$$L_d = -\frac{1}{2M} \sum_{i=0}^M [\log(1 - S_{AL}(p'_i)) + \log S_{AL}(p'_i + \delta_i)], \quad (10)$$

encourages the adaptor being sensitive to subtle changes on patch tokens, which may contribute to subtle anomaly localization. **(2) Anomaly localization on  $P'$ .** To encourage the adaptor to preserve abnormal features, we take the anomaly map predicted by the TFA on  $P$  as pseudo-labels:

$$L_p = -\frac{1}{M} \sum_{i=0}^M S_{AL}(p_i) \log(S_{AL}(p'_i)). \quad (11)$$

The overall learning objective to update  $\omega$  in our adaptor is  $L = L_d + L_p$ . This TTA is time-efficient and don't require any training data and annotation.

## Experiment

### Dataset.

We conduct zero-shot anomaly detection and localization experiments on two datasets: MVTEcAD (Bergmann et al. 2019) and VisA (Zou et al. 2022). MVTEc consists of data for 10 single objects and 5 textures, while VisA includes data

for 12 single or multiple object types. In this paper, only the test datasets are used for evaluating zero-shot anomaly detection and localization, and no additional datasets are used for all the methods.

### Metrics.

Following conventions in prior arts (Bergmann et al. 2019; Jeong et al. 2023), we use AUROC (Area Under the Receiver Operating Characteristic), F1Max, and PRO (Per-Region Overlap) to evaluate anomaly detection. Besides, we use AUROC, F1Max, and AUPR (Area Under the Precision-Recall curve) to evaluate anomaly localization.

### Implementation.

We adopt ViT-B-16+ (Dosovitskiy et al. 2020) as the visual encoder and the transformer (Vaswani et al. 2017) as the text encoder by default from the public pre-trained CLIP model (Ilharco et al. 2021). We also provide results under ResNet (He et al. 2016) and other ViT (Dosovitskiy et al. 2020) pre-trained models (Radford et al. 2021; Ilharco et al. 2021) in the supplementary material. For the visual encoder, we set the image size to  $240 \times 240$ , the same as the pre-training but without any image augmentation. For the text encoder, we use 22 base templates collected from CLIP, 7 pairs of contrastive state prompts, and 3 domain-aware prompts to generate sufficient prompts on the proposed template of domain-aware state prompting. All prompts are listed in the supplemental materials. For test-time adaptation, we use the AdamW optimizer and set the learning rate to 0.001. In addition, we optimize the adaptor with 5 epochs and report the mean and variance of the results over 5 random seeds.

### Performance

Table 1 and Table 2 present the performance of zero-shot anomaly localization and detection on MVTEcAD and VisA, respectively. We compare our proposed methods with prior vision-language based works, including vanilla CLIP (Radford et al. 2021), TransMM (Chefer, Gur, and Wolf 2021), MaskCLIP (Zhou, Loy, and Dai 2022), and WinCLIP (Jeong et al. 2023). Remarkably, both our proposed TFA and TTA show outstanding performance over other methods, significantly surpassing WinCLIP by margins of 5.5%, 4.8% and

AL	MVTecAD			VisA		
	Method	AUROC	F1Max	PRO	AUROC	F1Max
TransMM	57.5	12.1	21.9	49.4	14.8	10.2
MaskCLIP	63.7	18.5	40.5	60.9	7.3	27.3
WinCLIP	85.1	<u>31.7</u>	64.6	79.6	<u>14.8</u>	59.8
CLIP	19.5	6.2	1.6	22.3	1.4	0.8
+TFA(Ours)	<u>86.6</u>	30.1	<u>70.4</u>	<u>85.9</u>	14.7	<u>65.1</u>
+TTA(Ours)	<b>90.6±0.3</b>	<b>36.5±0.3</b>	<b>77.8±0.2</b>	<b>91.4±0.2</b>	<b>17.4±0.4</b>	<b>75.0±0.1</b>

Table 1: Zero-shot anomaly localization (AL) on MVTecAD and VisA. Bold indicates the best performance and underline indicates the runner-up unless other noted.

AD	MVTecAD			VisA		
	Method	AUROC	F1Max	AUPR	AUROC	F1Max
CLIP	74.0	88.5	89.1	59.3	74.4	67.0
WinCLIP	<u>91.8</u>	<u>92.9</u>	<u>96.5</u>	<u>78.1</u>	<u>79.0</u>	<u>81.2</u>
Ours	<b>92.5</b>	<b>93.2</b>	<b>96.7</b>	<b>79.2</b>	<b>79.7</b>	<b>81.7</b>

Table 2: Zero-shot anomaly detection (AD) performance on MVTecAD and VisA.

13.2% in terms of AUROC, F1Max, and PRO, respectively. In Fig. 4, we demonstrate the results of zero-shot anomaly localization. Both the visualizations and experimental results illustrate that our unified zero-shot anomaly localization model possesses the ability to effectively localize various types of defects across diverse samples.

## Ablation Studies

**Local-aware tokens extraction.** In table 3, we present an analysis of the impact derived from modifying the visual transformer within CLIP, a pivotal step towards acquiring local-aware tokens for anomaly localization. In comparison to the QKV attention mechanism in CLIP, the values (V) extracted from the final layer of the transformer as patch tokens shows basic anomaly localization capabilities. Notably, the patch tokens acquired through the residual accumulation of V-V attention across the multiple layers yield promising anomaly localization performance.

Architecture	AUROC	F1Max	PRO
with QKV attention	19.5	6.2	1.6
with V (last layer)	67.9	22.2	50.6
with V-V attention (last layer)	70.5	22.0	51.9
with V-V attention (multi-layer)	<b>86.6</b>	<b>30.1</b>	<b>70.4</b>

Table 3: Ablation studies on the attention adaptation of CLIP on MVTecAD. We denote query, key and value as Q, K and V, respectively.

**Prompt engineering.** Given the significance of language prompts in steering CLIP toward effective anomaly detection and localization, we undertake an analysis to the prompt engineering. The results of this examination are elaborated in Table 4. We collect some templates from CLIP to generate several prompts with "normal [class]" vs. "abnormal [class]". With these prompts, we employ a prompt ensemble strategy to carry out predictions. By designing multiple contrastive state prompts, we obtain a dramatic gain in both anomaly detection and localization. To keep a unified model, we essentially use generic state words, including pairs "perfect" vs. "imperfect", "blemished" vs. "unblemished", and other similar structures. Besides, domain-aware prompting enables the direct adaptation of text tokens to diverse data distributions, making a substantial contribution to the overall improvement in performance.

Prompt Eng.	Zero-shot A.D.			Zero-shot A.L.		
	Method	AUROC	F1Max	AUPR	AUROC	F1Max
Base	79.0	89.7	91.7	71.9	27.0	50.5
+CS Prompt	91.8	92.8	96.4	84.2	28.7	67.4
+DA Prompt	<b>92.5</b>	<b>93.2</b>	<b>96.7</b>	<b>86.6</b>	<b>30.1</b>	<b>70.4</b>

Table 4: Ablation studies on prompt engineering on MVTecAD. Note that our prompt engineering is also effective for anomaly detection (AD).

Adaptation	AUROC	F1Max	PRO
Linear Probe	88.9±0.1	33.1±0.2	74.4± 0.1
Ours	<b>90.6±0.3</b>	<b>36.5±0.3</b>	<b>77.8±0.2</b>

Table 5: Ablation on adapter optimization on MVTecAD.

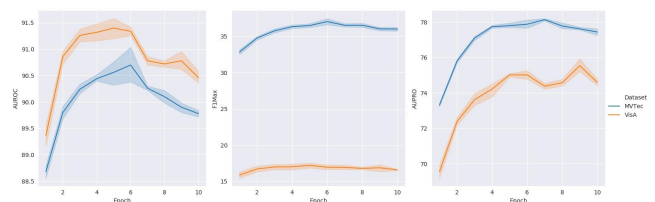


Figure 5: Ablation on TTA epochs on MVTecAD and VisA.

**Test-time adaptation with dual-task optimization.** The CLIP-Adapter (Gao et al. 2021) proposed to fine-tune a linear probe on few samples for image recognition. Nevertheless, our test-time adaptation exhibits only marginal improvement when employed with the linear probe for  $\omega$  optimization, due to poor random initialization. Therefore, we propose to use the text tokens to initiate the weights in this study. Table 5 shows that our adapter optimized by the proposed dual tasks brings a great performance improvement compared to the linear probe. Additionally, we visualize the

Setting	Full-shot							Zero-shot		
	Method	US	PSVDD	PaDiM	CutPaste	FCDD	MKD	DRAEM	UniAD	WinCLIP
AD	74.5	76.8	84.2	77.5	-	81.9	88.1	<b>96.5+0.1</b>	91.2	<u>92.5+0.0</u>
AL	81.8	85.6	89.5	-	63.3	84.9	87.2	<b>96.8+0.0</b>	85.1	<u>90.6+0.3</u>

Table 6: Comparison of multi-class anomaly detection and localization performance on MVTEC. We compare the performance of our zero-shot approach to the state-of-the-art full-shot unified model UniAD (You et al. 2022) on MVTEcAD, as well as US (Bergmann et al. 2020), PSVDD (Yi and Yoon 2020), PaDiM (Defard et al. 2021), CutPaste (Li et al. 2021), FCDD (Liznerski et al. 2020), MKD (Salehi et al. 2021b), and DRAEM (Zavrtanik, Kristan, and Skočaj 2021) on the multi-class task. Full-shot results are taken from UniAD (You et al. 2022).

impact of running epochs on performance in Fig. 5. As the number of running epochs increases, our test-time adaptation shows a trend of convergence. While a slight performance decrease is observed as the number of iterations increases, it’s important to note that test-time adaptation often involves a limited number of epochs due to time constraints. Considering the trade-off between performance and time cost, we exclusively run 5 epochs for test-time adaptation within our experiments.

**TFA vs. TTA** We show the patch tokens virtualisation of TFA and TTA processed by t-SNE (Van der Maaten and Hinton 2008) in Figure 6. In this case, TFA shows no tendency to some anomalous tokens, while TTA refines them to yield more precise results.

**Model Efficiency.** In Table 7, we present the zero-shot anomaly localization efficiency concerning performance and inference time. Our TFA for CLIP with only 1.4 ms increase in inference time exceeds the performance of WinCLIP, which is time-consuming because of the multi-scale window moving operation. polish this: TTA yields a significant performance boost at the cost of  $3\times$  time consumption compared to TFA, while still more efficient than WinCLIP.

Methods	AUROC	F1Max	PRO	Time (ms)
WinCLIP	85.1	<u>31.7</u>	79.6	41.3±1.2
CLIP	19.5	6.2	1.6	<b>6.2±0.2</b>
+TFA(Ours)	<u>86.6</u>	30.1	<u>70.4</u>	<u>7.6±0.2</u>
+TTA(Ours)	<b>90.6±0.3</b>	<b>36.5±0.3</b>	<b>77.8±0.2</b>	20.1±1.4

Table 7: Comparison of model efficiency. We measure the inference time per image with an RTX3090 GPU.

## Limitations and conclusion

**Limitations** While we achieve truly unified anomaly detection and localisation and SOTA performance in the zero-shot setting, there is still a gap compared to the SOTA model trained in the full-shot manner. As shown in Table 6, our zero-shot approach surpasses most of the models on multi-class anomaly detection and localization. However, we underperform the UniAD (You et al. 2022), which achieves the best results by training on multi-class normal datasets.

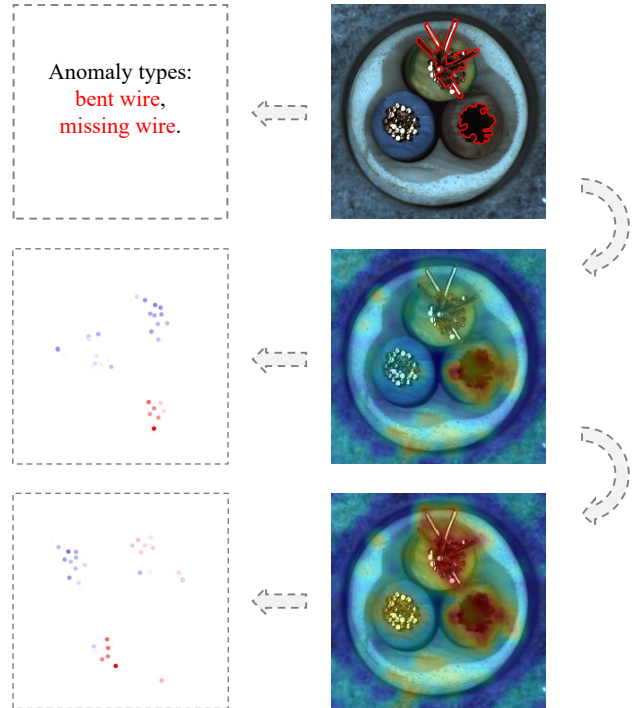


Figure 6: t-SNE visualization on TFA and TTA. The sample is from "cable" class in MVTEcAD and has two anomaly types: bent wire and missing wire. Red indicates abnormal state and blue indicates normal state, while the shade represent the anomaly score.

Therefore, our future work is to fine tune visual language models on some normal data, such as few-shot and full-shot, to achieve better performance.

**Conclusion** We introduce a novel framework aimed at resolving unified zero-shot anomaly detection and localization. Through adapting the vision-language models such as CLIP, we achieve state-of-the-art performance without any training dataset. We first extract implicitly local-aware tokens from CLIP for precise anomaly localization. Then, we propose a domain-aware state prompt template for generating sufficient and effective prompts. Finally, we use test-time adaptation to refine features to localize anomalies more pre-

cisely. This study demonstrates that visual language models are able to solve unified anomaly detection and localization problems without being constrained by training data.

## References

- Aota, T.; Tong, L. T. T.; and Okatani, T. 2023. Zero-shot versus many-shot: Unsupervised texture anomaly detection. In *Proceedings of the IEEE/CVF Winter Conference on Applications of Computer Vision*, 5564–5572.
- Bergmann, P.; Fauser, M.; Sattlegger, D.; and Steger, C. 2019. MVTEC AD—A comprehensive real-world dataset for unsupervised anomaly detection. In *Proceedings of the IEEE/CVF conference on computer vision and pattern recognition*, 9592–9600.
- Bergmann, P.; Fauser, M.; Sattlegger, D.; and Steger, C. 2020. Uninformed students: Student-teacher anomaly detection with discriminative latent embeddings. In *Proceedings of the IEEE/CVF conference on computer vision and pattern recognition*, 4183–4192.
- Chefer, H.; Gur, S.; and Wolf, L. 2021. Generic attention-model explainability for interpreting bi-modal and encoder-decoder transformers. In *Proceedings of the IEEE/CVF International Conference on Computer Vision*, 397–406.
- Chen, Y.-C.; Li, L.; Yu, L.; El Kholy, A.; Ahmed, F.; Gan, Z.; Cheng, Y.; and Liu, J. 2020. Uniter: Universal image-text representation learning. In *European conference on computer vision*, 104–120. Springer.
- Cohen, N.; Abutbul, R.; and Hoshen, Y. 2022. Out-of-Distribution Detection without Class Labels. In *European Conference on Computer Vision*, 101–117. Springer.
- Defard, T.; Setkov, A.; Loesch, A.; and Audigier, R. 2021. Padim: a patch distribution modeling framework for anomaly detection and localization. In *International Conference on Pattern Recognition*, 475–489. Springer.
- Deng, H.; and Li, X. 2022. Anomaly detection via reverse distillation from one-class embedding. In *Proceedings of the IEEE/CVF Conference on Computer Vision and Pattern Recognition*, 9737–9746.
- Deng, J.; Dong, W.; Socher, R.; Li, L.-J.; Li, K.; and Fei-Fei, L. 2009. Imagenet: A large-scale hierarchical image database. In *2009 IEEE conference on computer vision and pattern recognition*, 248–255. Ieee.
- Desai, K.; and Johnson, J. 2021. Virtex: Learning visual representations from textual annotations. In *Proceedings of the IEEE/CVF conference on computer vision and pattern recognition*, 11162–11173.
- Dosovitskiy, A.; Beyer, L.; Kolesnikov, A.; Weissenborn, D.; Zhai, X.; Unterthiner, T.; Dehghani, M.; Minderer, M.; Heigold, G.; Gelly, S.; et al. 2020. An image is worth 16x16 words: Transformers for image recognition at scale. *arXiv preprint arXiv:2010.11929*.
- Gao, P.; Geng, S.; Zhang, R.; Ma, T.; Fang, R.; Zhang, Y.; Li, H.; and Qiao, Y. 2021. Clip-adapter: Better vision-language models with feature adapters. *arXiv preprint arXiv:2110.04544*.
- Gu, X.; Lin, T.-Y.; Kuo, W.; and Cui, Y. 2021. Open-vocabulary object detection via vision and language knowledge distillation. *arXiv preprint arXiv:2104.13921*.
- He, K.; Zhang, X.; Ren, S.; and Sun, J. 2016. Deep residual learning for image recognition. In *Proceedings of the IEEE conference on computer vision and pattern recognition*, 770–778.
- Huang, C.; Guan, H.; Jiang, A.; Zhang, Y.; Spratling, M.; and Wang, Y.-F. 2022. Registration based few-shot anomaly detection. In *European Conference on Computer Vision*, 303–319. Springer.
- Ilharco, G.; Wortsman, M.; Wightman, R.; Gordon, C.; Carlini, N.; Taori, R.; Dave, A.; Shankar, V.; Namkoong, H.; Miller, J.; Hajishirzi, H.; Farhadi, A.; and Schmidt, L. 2021. OpenCLIP. If you use this software, please cite it as below.
- Jeong, J.; Zou, Y.; Kim, T.; Zhang, D.; Ravichandran, A.; and Dabeer, O. 2023. Winclip: Zero-/few-shot anomaly classification and segmentation. In *Proceedings of the IEEE/CVF Conference on Computer Vision and Pattern Recognition*, 19606–19616.
- Joulin, A.; Van Der Maaten, L.; Jabri, A.; and Vasilache, N. 2016. Learning visual features from large weakly supervised data. In *Computer Vision—ECCV 2016: 14th European Conference, Amsterdam, The Netherlands, October 11–14, 2016, Proceedings, Part VII 14*, 67–84. Springer.
- Kuo, W.; Cui, Y.; Gu, X.; Piergiovanni, A.; and Angelova, A. 2022. F-vlm: Open-vocabulary object detection upon frozen vision and language models. *arXiv preprint arXiv:2209.15639*.
- Li, C.-L.; Sohn, K.; Yoon, J.; and Pfister, T. 2021. Cutpaste: Self-supervised learning for anomaly detection and localization. In *Proceedings of the IEEE/CVF conference on computer vision and pattern recognition*, 9664–9674.
- Li, Y.; Wang, H.; Duan, Y.; and Li, X. 2023. Clip surgery for better explainability with enhancement in open-vocabulary tasks. *arXiv preprint arXiv:2304.05653*.
- Liu, W.; Luo, W.; Lian, D.; and Gao, S. 2018. Future frame prediction for anomaly detection—a new baseline. In *Proceedings of the IEEE conference on computer vision and pattern recognition*, 6536–6545.
- Liu, Z.; Zhou, Y.; Xu, Y.; and Wang, Z. 2023. SimpleNet: A Simple Network for Image Anomaly Detection and Localization. In *Proceedings of the IEEE/CVF Conference on Computer Vision and Pattern Recognition (CVPR)*, 20402–20411.
- Liznerski, P.; Ruff, L.; Vandermeulen, R. A.; Franks, B. J.; Kloft, M.; and Müller, K.-R. 2020. Explainable deep one-class classification. *arXiv preprint arXiv:2007.01760*.
- Ming, Y.; Cai, Z.; Gu, J.; Sun, Y.; Li, W.; and Li, Y. 2022. Delving into out-of-distribution detection with vision-language representations. *Advances in Neural Information Processing Systems*, 35: 35087–35102.
- Radford, A.; Kim, J. W.; Hallacy, C.; Ramesh, A.; Goh, G.; Agarwal, S.; Sastry, G.; Askell, A.; Mishkin, P.; Clark, J.; et al. 2021. Learning transferable visual models from natural language supervision. In *International conference on machine learning*, 8748–8763. PMLR.



- Roth, K.; Pemula, L.; Zepeda, J.; Schölkopf, B.; Brox, T.; and Gehler, P. 2022. Towards total recall in industrial anomaly detection. In *Proceedings of the IEEE/CVF Conference on Computer Vision and Pattern Recognition*, 14318–14328.
- Salehi, M.; Sadjadi, N.; Baselizadeh, S.; Rohban, M. H.; and Rabiee, H. R. 2021a. Multiresolution Knowledge Distillation for Anomaly Detection. In *Proceedings of the IEEE/CVF Conference on Computer Vision and Pattern Recognition (CVPR)*, 14902–14912.
- Salehi, M.; Sadjadi, N.; Baselizadeh, S.; Rohban, M. H.; and Rabiee, H. R. 2021b. Multiresolution knowledge distillation for anomaly detection. In *Proceedings of the IEEE/CVF conference on computer vision and pattern recognition*, 14902–14912.
- Schlegl, T.; Seeböck, P.; Waldstein, S. M.; Langs, G.; and Schmidt-Erfurth, U. 2019. f-AnoGAN: Fast unsupervised anomaly detection with generative adversarial networks. *Medical image analysis*, 54: 30–44.
- Schwartz, E.; Arbelle, A.; Karlinsky, L.; Harary, S.; Scheidegger, F.; Doveh, S.; and Giryas, R. 2022. MAEDAY: MAE for few and zero shot Anomaly-Detection. *arXiv preprint arXiv:2211.14307*.
- Shin, G.; Xie, W.; and Albanie, S. 2022. Reco: Retrieve and co-segment for zero-shot transfer. *Advances in Neural Information Processing Systems*, 35: 33754–33767.
- Shu, M.; Nie, W.; Huang, D.-A.; Yu, Z.; Goldstein, T.; Anandkumar, A.; and Xiao, C. 2022. Test-time prompt tuning for zero-shot generalization in vision-language models. *Advances in Neural Information Processing Systems*, 35: 14274–14289.
- Van der Maaten, L.; and Hinton, G. 2008. Visualizing data using t-SNE. *Journal of machine learning research*, 9(11).
- Vaswani, A.; Shazeer, N.; Parmar, N.; Uszkoreit, J.; Jones, L.; Gomez, A. N.; Kaiser, Ł.; and Polosukhin, I. 2017. Attention is all you need. *Advances in neural information processing systems*, 30.
- Yi, J.; and Yoon, S. 2020. Patch svdd: Patch-level svdd for anomaly detection and segmentation. In *Proceedings of the Asian conference on computer vision*.
- You, Z.; Cui, L.; Shen, Y.; Yang, K.; Lu, X.; Zheng, Y.; and Le, X. 2022. A unified model for multi-class anomaly detection. *Advances in Neural Information Processing Systems*, 35: 4571–4584.
- Zagoruyko, S.; and Komodakis, N. 2016. Wide residual networks. *arXiv preprint arXiv:1605.07146*.
- Zavrtanik, V.; Kristan, M.; and Skočaj, D. 2021. DRAEM - A Discriminatively Trained Reconstruction Embedding for Surface Anomaly Detection. In *Proceedings of the IEEE/CVF International Conference on Computer Vision (ICCV)*, 8330–8339.
- Zhang, R.; Fang, R.; Zhang, W.; Gao, P.; Li, K.; Dai, J.; Qiao, Y.; and Li, H. 2021. Tip-adapter: Training-free clip-adapter for better vision-language modeling. *arXiv preprint arXiv:2111.03930*.
- Zhou, B.; Khosla, A.; Lapedriza, A.; Oliva, A.; and Torralba, A. 2016. Learning deep features for discriminative localization. In *Proceedings of the IEEE conference on computer vision and pattern recognition*, 2921–2929.
- Zhou, C.; Loy, C. C.; and Dai, B. 2022. Extract free dense labels from clip. In *European Conference on Computer Vision*, 696–712. Springer.
- Zhou, K.; Yang, J.; Loy, C. C.; and Liu, Z. 2022a. Conditional prompt learning for vision-language models. In *Proceedings of the IEEE/CVF Conference on Computer Vision and Pattern Recognition*, 16816–16825.
- Zhou, K.; Yang, J.; Loy, C. C.; and Liu, Z. 2022b. Learning to prompt for vision-language models. *International Journal of Computer Vision*, 130(9): 2337–2348.
- Zou, Y.; Jeong, J.; Pemula, L.; Zhang, D.; and Dabeer, O. 2022. Spot-the-difference self-supervised pre-training for anomaly detection and segmentation. In *European Conference on Computer Vision*, 392–408. Springer.